Supplementary Material

Supplementary Table S1: Study sites, coordinates, and geological characteristics, and corresponding site-specific publications.

Loc. No.	Location (short code) Site specific references	Sampling year	Age (kyr)	°N	°E	bedrock/ parent rock
1	Bol'shoy Lyakhovsky Island (Zimov'e River, L, R, TZ, L7) (Andreev et al., 2004, 2009; Boike et al., 2008; Kienast et al., 2008; Kunitsky et al., 2002; Kusch et al., 2019; Meyer et al., 2002a; Palagushkina et al., 2012, 2017; Schennen et al., 2016; Schirrmeister et al., 2000, 2002c; Schwamborn et al., 2015; Stapel et al., 2018; Walz et al., 2018; Wetterich et al., 2009, 2011, 2014, 2016, 2019, 2021; Zimmermann et al., 2017)	1999, 2007	54 - 22	73.30	141.5	Permian to Triassic siltstone, sandstone, mudstone, Early Cretaceous granite
2	Oyogos Yar coast (Oy7) (Boike et al., 2008; Grigoriev et al., 2003; Kienast et al., 2011; Opel et al., 2010, 2017; Schirrmeister et al., 2011b; Wetterich et al., 2009, 2014, 2016)	2007	48 - 32	72.68	143.53	Neogene silt, sand, and gravel

3	Cape Svyatoy Nos (X-99) (Schirrmeister et al., 2011b)	1999	>50 - 36	72.84	140.85	Cretaceous granite
4	Stolbovoy Island (Sto) (Grigoriev et al., 2003; Schirrmeister et al., 2011b)	2002	>51 – 36.6	74.06	136.08	Cretaceous sandstone, siltstone
5	Bel'kovskiy Island (Bel) (Grigoriev et al., 2003; Schirrmeister et al., 2011b)	2002	54 - 40	75.37	135.59	Devonian siltstone, mudstone, sandstone, limestone
6	Cape (Mys) Anisii, northern Kotel'ny Island, (Mya) (Grigoriev et al., 2003; Schirrmeister et al., 2011b)	2002	28	76.17	139.01	Silurian limestone, siltstone
7	Bunge Land (Bun) (Grigoriev et al., 2003; Schirrmeister et al., 2010)	2002	12.5 – 7 modern	74.87 74.84	142.16 140.39	Triassic and Devonian silt, sand, and limestone
8	Novaya Sibir Island (Nes) (Grigoriev et al., 2003)	2002	> 52 - 9	75.12	146.65	Tertiary sand, gravel, silt Jurassic silt, clay, sandstone
9	Mamontovy Khayata, Bykovsky Peninsula (Mkh) (Andreev et al., 2002; Bobrov et al., 2003, 2004; Grosse et al., 2005, 2007; Kienast et al., 2005; Kuznetsova et al., 2019; Meyer et al., 2000; Schirrmeister et al., 2002a, b; Sher et al., 2000, 2005; Siegert et al., 1999; 2002; Wetterich et al., 2005)	1998, 1999	57 - 12	71.78	129.43	Permocarbon sandstone and slate of the Kharaulakh Range
10	Bykovsky North, Bykovsky Peninsula (B-S) (Siegert et al., 1999)	1998	53 – 13.4	71.95	129.19	Permocarbon sandstone and slate of the Kharaulakh Range

11	Ivashkina Lagoon, Bykovsky Peninsula (Iv-2-99) (Schwamborn et al., 2000; Schirrmeister et al., 2018)	1999	36 – 0.5	71.74	129.40	Permocarbon sandstone and slate of the Kharaulakh Mountain + Surrounding Yedoma Ice Complex
12	Khorogor Valley (Khg) (Grigoriev et al., 2003; Grosse et al., 2007)	2002	modern	71.73	128.72	Permocarbon sandstone and slate of the Kharaulakh Mountain
13	Ebe Basyn Island (Ebe) (Schirrmeister et al., 2007, 2011a)	2005	12.6 – 0.6	72.93	123.60	Mesozoic sandstone and slate of the Chekanovsky Ridge
14	Turakh Island, Arga Complex (Tur) (Schirrmeister et al., 2007, 2011a)	2005	> 52 – 0.3	72.97	123.80	Paleo Lena River deposits
15	Nagym, Ebe Basyn Island (Nag) (Schirrmeister et al., 2001, 2003, 2011a)	2000	>56.8 - 43	72.88	123.32	Paleo Lena River deposits
16	Khardang Island (Kha) (Schirrmeister et al., 2007, 2011a)	2005	30 - 20	72.95	124.21	Paleo Lena River deposits
17	Kurungnakh Island (Bkh) (Schirrmeister et al., 2001, 2003, 2011a; Schwamborn et al., 2002; Wetterich et al., 2008)	2002	50 - 32	72.33	126.30	Paleo Lena River deposits and Mesozoic sandstone and slate of the Chekanovsky Ridge
18	Cape Mamontov Klyk (Mak) (Bobrov et al., 2009; Grosse et al., 2006; Mitzscherling et al., 2019; Müller et al., 2009; Schirrmeister et al., 2004, 2008; Winterfeld et al., 2011)	2003	46 - 9.5	73.61	117.18	Mesozoic sandstone and siltstone of the Pronchishchev Range

References

Andreev, A.A., Schirrmeister, L., Siegert, C., Bobrov, A.A., Demske, D., Seiffert, M., and Hubberten, H.-W. (2002). Paleoenvironmental changes in Northeastern Siberia during the Late Quaternary - evidence from pollen records of the Bykovsky Peninsula. *Polarforschung* 70, 13-25, doi: 10.2312/polarforschung.70.13

Andreev, A.A., Grosse, G., Schirrmeister, L., Kuzmina, S.A., Novenko, E.Yu., Bobrov, A.A., Tarasov, P. E., Kuznetsova, T.V., Krbetschek, M., Meyer, H., and Kunitsky, V.V. (2004). Late Saalian and Eemian palaeoenvironmental history of the Bol'shoy Lyakhovsky Island (Laptev Sea region, Arctic Siberia). *Boreas* 33(4), 319-348, doi: 10.1080/03009480410001974

Andreev, A., Grosse, G., Schirrmeister, L., Kuznetsova, T.V., Kuzmina, S.A., Bobrov, A.A., Tarasov, P.E., Novenko, E.Yu., Meyer, H., Derevyagin, A.Yu., Kienast, F., Bryantseva, A., and Kunitsky, V.V. (2009). Weichselian and Holocene palaeoenvironmental history of the Bol'shoy Lyakhovsky Island, New Siberian Archipelago, Arctic Siberia, *Boreas* 38(1), 72–110, doi: 10.1111/j.1502-3885.2008.00039.x

Boike, J., Bolshiyanov, D.Yu., Schirrmeister, L., and Wetterich, S. (eds., 2008). Russian-German Cooperation SYSTEM LAPTEV SEA: The Expedition Lena - New Siberian Islands 2007 during the International Polar Year (IPY) 2007/2008. *Reports on Polar and Marine Research* 584, 265 pp., doi: 10.2312/BzPM_0584_2008

Bobrov, A.A., Siegert, Ch., Andreev, A.A., and Schirrmeister, L. (2003). Testaceans (Protozoa: Testacea) in Quaternary permafrost sediments of Bykovsky Peninsula, Arctic Yakutia. *Biology Bulletin* 30(2), 191-206, doi: 10.1023/A:1023201624996

Bobrov, A.A., Andreev, A.A., Schirrmeister, L., and Siegert, Ch. (2004). Testate amoebae (Protozoa: Testacea) as bioindicators in the Late Quaternary deposits of the Bykovsky Peninsula, Laptev Sea, Russia, *Palaeogeography palaeoclimatology palaeoecology* 209, 165-181. doi: 10.1016/J.PALAEO.2004.02.012

Bobrov, A.A., Müller, S., Chizhikova, N.A., Schirrmeister, L., and Andreev, A.A. (2009). Testate Amoebae in Late Quaternary Sediments of the Cape Mamontov Klyk (Yakutia). *Biology Bulletin* 36(4), 363-372, doi: 10.1134/S1062359009040074

Grigoriev, M. N., Rachold, V., Bolshiyanov, D. Yu., Pfeiffer, E.-M., Schirrmeister, L., Wagner, D., and Hubberten, H.-W. (eds., 2003). Russian-German Cooperation System Laptev Sea - The Expedition Lena 2002. *Reports on Polar and Marine Research* 466, 341 pp., doi: 10.2312/BzPM_0466_2003

Grosse, G., Schirrmeister, L., Kunitsky, V.V., and Hubberten, H.-W. (2005). The Use of CORONA Images in Remote Sensing of Periglacial Geomorphology: An Illustration from the NE Siberian Coast. *Permafrost and periglacial processes* 16, 163-172, doi: 10.1002/ppp.509

Grosse, G., Schirrmeister, L., and Malthus, T.J. (2006). Application of Landsat-7 satellite data and a DEM for the quantification of thermokarst-affected terrain types in the periglacial Lena-Anabar coastal lowland. *Polar research* 25(1), 51-67, doi: 10.3402/polar.v25i1.6238

Grosse, G., Schirrmeister, L., Siegert, C., Kunitsky, V.V., Slagoda, E.A., Andreev, A.A., and Dereviagyn, A.Y. (2007). Geological and geomorphological evolution of a sedimentary periglacial landscape in Northeast Siberia during the Late Quaternary. *Geomorphology* 86(1/2), 25-51, doi: 10.1016/j.geomorph.2006.08.005

Kienast, F., Schirrmeister, L., Siegert, C., and Tarasov, P. (2005). Palaeobotanical evidence for warm summers in the East Siberian Arctic during the last cold stage. *Quaternary Research* 63(3), 283-300, doi: 10.1016/j.yqres.2005.01.003

Kienast, F., Tarasov, P., Schirrmeister, L., Grosse, G., and Andreev, A.A. (2008). Continental climate in the East Siberian Arctic during the last interglacial: implications from palaeobotanical records. *Global and Planetary Change* 60(3/4), 535-562, doi: 10.1016/j.gloplacha.2007.07.004

Kienast, F., Wetterich, S., Kuzmina, S., Schirrmeister, L., Andrev, A., Tarasov, P., Nazarova, L., Kossler, A., Frolova, A., and Kunitsky, V.V. (2011). Paleontological records indicate the occurrence of open woodlands in a dry inland climate at the present-day Arctic coast in western Beringia during the last interglacial. *Quaternary Science Reviews* 30, 2134-2159, doi: 10.1016/j.quascirev.2010.11.024

Kunitsky, V., Schirrmeister, L., Grosse, G., Kienast, F. (2002). Snow patches in nival landscapes and their role for the Ice Complex formation in the Laptev Sea coastal lowlands. *Polarforschung* 70, 53-67, doi:10.2312/polarforschung.70.53

Kusch, S., Winterfeld, M., Mollenhauer, G., Höfle, S.T., Schirrmeister, L., Schwamborn, G., and Rethemeyer, J. (2019). Glycerol dialkyl glycerol tetraethers (GDGTs) in high latitude Siberian permafrost: Diversity, environmental controls, and implications for proxy applications. *Organic Geochemistry* 136, 103888, doi: 10.1016/j.orggeochem.2019.06.009

Kuznetsova T.V., Tumskoy V.E., Schirrmeister L., Wetterich S. (2019). Paleozoological characteristics of the Late Neo-Pleistocene - Holocene sediments of Bykovsky Peninsula, Northern Yakutia. *Zoological Journal* 98(11), 1268-1290. Special issue in honor of Andrey Sher. (in Russian), doi: 10.1134/S0044513419110102

Meyer, H., Schönicke, L., Wand, U., Hubberten, H. W. and Friedrichsen, H. (2000). Isotope studies of hydrogen and oxygen in ground ice experiences with the equilibration technique. *Isotopes in Environmental and Health Studies* 36, 133-149, doi: 10.1080/10256010008032939

Meyer, H., Dereviagin, A. Yu., Siegert, C., Schirrmeister, L., and Hubberten, H.-W. (2002a). Paleoclimate reconstruction on Big Lyakhovsky Island, North Siberia - Hydrogen and oxygen isotopes in ice wedges. *Permafrost and periglacial processes* 13, 91-105. doi: 10.1002/ppp.416

Meyer, H., Derevyagin, A. Y., Siegert, C. and Hubberten, H. W. (2002b) Paleoclimate studies on Bykovsky Peninsula, North Siberia - hydrogen and oxygen isotopes in ground ice. *Polarforschung* 70, 37-51, doi:10.2312/polarforschung.70.37

Mitzscherling, J., Horn, F., Winterfeld, M., Mahler, L., Kallmeyer, J., Overduin, P.P., Schirrmeister, L., Winkel, M., Grigoriev, M.N., Wagner, D., and Liebner, S. (2019). Microbial community composition and abundance after millennia of submarine permafrost warming. *Biogeosciences* 16, 3941–3958, doi: 10.5194/bg-16-3941-2019

Müller, S., Bobrov, A. A., Schirrmeister, L., Andreev, A. A., and Tarasov, P. E. (2009). Testate amoebae record from the Laptev Sea coast and its implication for the reconstruction of Late Pleistocene and Holocene environments in the Arctic Siberia. *Palaeogeography, Palaeoclimatology, Palaeoecology* 271(3-4), 301-315. doi: 10.1016/j.palaeo.2008.11.003

Opel, T., Dereviagin, A., Meyer, H., Schirrmeister, L., and Wetterich, S. (2010.) Paleoclimatic information from stable water isotopes of Holocene ice wedges at the Dmitrii Laptev Strait (Northeast Siberia). *Permafrost and Periglacial Processes* 22 (1), 84-100, doi: 10.1002/ppp.667

Opel, T., Wetterich, S., Meyer, H., Dereviagin, A.Yu., Fuchs, M.C., and Schirrmeister, L. (2017). Ground-ice stable isotopes and cryostratigraphy reflect late Quaternary palaeoclimate in the Northeast Siberian Arctic (Oyogos Yar coast, Dmitry Laptev Strait). *Clim. Past* 13, 587–611, doi: 10.5194/cp-13-587-2017

Palagushkina, O.V., Wetterich, S., Schirrmeister, L., and Nazarova, L.B. (2017). Modern and fossil diatom assemblages from Bol'shoy Lyakhovsky Island (New Siberian Archipelago, Arctic Siberia). *Contemporary Problems of Ecology* 10(4), 380–394. doi: 10.1134/S1995425517040060

Palagushkina, O., Nazarova, L., Wetterich, S. and Schirrmeister, L. (2012). Diatoms of Modern Bottom Sediments in Siberian Arctic. *Contemporary Problems of Ecology* 5(4), 413-422, doi: 10.1134/S1995425512040105

Schennen, S., Tronicke, J., Wetterich, S., Allroggen, N., Schwamborn, G., and Schirrmeister, L. (2016). 3D GPR imaging of Ice Complex deposits in northern East Siberia. *Geophysics* 81(1), WA185-WA192, doi: 10.1190/GEO2015-0129.1

Schirrmeister, L., Kunitsky, V., Grosse, V., Meyer, H., Kuznetsova, T., Kuzmina, S., Tumskoy, V., Derevyagin, A., Akhmadeeva, I., and Syromyatnikov, I. (2000). Quaternary deposits of Bol'shoy Lyakhovsky Island. *Reports on Polar and Marine Research* 354, 113-168, doi: 10.2312/BzP_0354_1_2000

Schirrmeister, L., Kunitsky, V., Grosse, G., Kuznetsova, T., Kuzmina, S., and Bolshianov, D. (2001). Late Quaternary and recent environmental situation around the Olenyok Channel (western Lena Delta) and on Bykovsky Peninsula. *Reports on Polar and Marine Research* 388, 85-135, doi: 10.2312/BzPM_0388_2001

Schirrmeister, L., Siegert, C., Kuznetsova, T., Kuzmina, S., Andreev, A.A., Kienast, F., Meyer, H., and Bobrov, A.A. (2002a). Paleoenvironmental and paleoclimatic records from permafrost deposits in the Arctic region of Northern Siberia. *Quaternary International* 89, 97-118, doi: 10.1016/S1040-6182(01)00083-0

Schirrmeister, L., Siegert, C., Kunitzky, V.V., Grootes, P.M., and Erlenkeuser, H. (2002b). Late Quaternary ice-rich permafrost sequences as a paleoenvironmental archive for the Laptev Sea Region in northern Siberia. *International Journal of Earth Sciences* 91, 154-167, doi: 10.1007/s005310100205

Schirrmeister, L., Oezen, D., and Geyh, M.A. (2002c). 230Th/U dating of frozen peat, Bol'shoy Lyakhovsky Island (North Siberia). *Quaternary research* 57, 253-258. doi: 10.1006/qres.2001.2306

Schirrmeister, L., Kunitsky, V.V., Grosse, G., Schwamborn, G., Andreev, A.A., Meyer, H., Kuznetsova, T., Bobrov, A., and Oezen, D. (2003). Late Quaternary history of the accumulation plain north of the Chekanovsky Ridge (Lena Delta, Russia) - a multidisciplinary approach. *Polar Geography* 27(4), 277-319, doi: 10.1080/789610225

Schirrmeister, L., Grigoriev, M.N., Kutzbach, L., Wagner, D., and Bolshiyanov, D.Yu. (2004). Russian-German Cooperation SYSTEM Laptev Sea: The Expedition Lena-Anabar 2003. *Reports on Polar and Marine Research* 489, 1-209, doi: https://doi.org/10.2312/BzPM_0489_2004

Schirrmeister, L., Wagner, D, Grigoriev, M.N., and Bolshiyanov, D.Y. (eds.): The Expedition LENA 2005, Expeditions in Siberia in 2005, ed. by Lutz Schirrmeister, Reports on Polar and Marine Research, 550, 41-242, doi.org/10.2312/BzPM_0550_2007, 2007.

Schirrmeister, L., Grosse, G., Kunitsky, V., Magens, D., Meyer, H., Dereviagin, A., Kuznetsova, T., Andreev, A., Babiy, O., Kienast, F., Grigoriev, M., Overduin, P.P., and Preusser, F. (2008). Periglacial landscape evolution and environmental changes of Arctic lowland areas for the last 60,000 years (Western Laptev Sea coast, Cape Mamontov Klyk). *Polar Research* 27(2), 249-272, doi: 10.1111/j.1751-8369.2008.00067.x

Schirrmeister, L., Grosse, G., Kunitsky, V.V., Fuchs, M.C., Krbetschek, M., Andreev, A.A., Herzschuh, U., Babiy, O., Siegert, C., Meyer, H., Derevyagin, A.Y., and Wetterich S. (2010). The mystery of Bunge Land (New Siberian Archipelago): Implications for its formation based on palaeo-environmental records, geomorphology, and remote sensing. *Quaternary Science reviews* 29, 3598–3614. doi: 10.1016/j.quascirev.2009.11.017

Schirrmeister, L., Grosse, G. Schnelle, M., Fuchs, M., Krbetschek, M., Ulrich, M., Kunitsky, V., Grigoriev, M., Andreev, A. Kienast, F., Meyer, H., Klimova, I., Babiy, O., Bobrov, A., Wetterich,

S., and Schwamborn, G. (2011a). Late Quaternary paleoenvironmental records from the western Lena Delta, Arctic Siberia. *Palaeogeography, Palaeoclimatology, Palaeoecology* 299, 175–196, doi: 10.1016/j.quascirev.2009.11.017

Schirrmeister, L., Kunitsky, V.V., Grosse, G., Wetterich, S., Meyer, H., Schwamborn, G., Babiy, O., Derevyagin, A.Y., and Siegert, C. (2011b). Sedimentary characteristics and origin of the Late Pleistocene Ice Complex on North-East Siberian Arctic coastal lowlands and islands - a review. *Quaternary International* 241, 3-25, doi: 10.1016/j.quaint.2010.04.004

Schirrmeister, L., Grigoriev, M.N., Strauss, J., Grosse, G., Overduin, P.P., Kholodov, A., Guenther, F., and Hubberten, H.-W. (2018). Sediment characteristic of a thermokarst lagoon in the Northeast Siberian Arctic (Ivashkina Lagoon, Bykovsky Peninsula. *Arktos* 4(13), 1-16,. doi: 10.1007/s41063-018-0049-8,

Schwamborn, G, Bolshiyanov, D.Yu, Dorozhkina, M., Grigoriev, M.N., Pavolva, E.Yu, Schneider, W., and Tumskoy, V.E. (2000). Lake Sediment Studies on Arga Island. *Reports on Polar Research* 354, 57-54, doi: 10.2312/BzP_0354_1_2000

Schwamborn, G., Rachold, V., and Grigoriev, M.N. (2002).Late Quaternary sedimentation history of the Lena Delta. *Quaternary International* 89, 119–134, doi: 10.1016/S1040-6182(01)00084-2

Schwamborn, G., and Wetterich, S. (eds., 2015). Russian-German Cooperation CARBOPERM: Field campaigns to Bol'shoy Lyakhovsky Island in 2014. *Reports on Polar and Marine Research* 686, 1-98, doi: 10.2312/BzPM_0686_20152015

Sher, A., Parmuzin, I., and Bortsov, A. (2000). Ice complex on the Bykovsky Peninsula, in Russian–German Cooperation System Laptev Sea 2000: The Expedition LENA 1999. *Reports on Polar and Marine Research* 354, 169–182, doi: 10.2312/BzP_0354_1_2000

Sher, A.V., Kuzmina, S.A., Kuznetsova, T.V., and Sulerzhitsky, L.D. (2005). New insights into the Weichselian environment and climate of the East Siberian Arctic, derived from fossil insects, plants, and mammals. *Quaternary Science Reviews* 24, 533–569, doi: 10.1016/j.quascirev.2004.09.007

Siegert, C., Schirrmeister, L., Kunitsky, V., Meyer, H., Kuznetsova, T., Derevyagin, S., Kuzmina, S., Tumskoy, V., and Sher, A. (1999). Paleoclimate signals of ice-rich permafrost. *Reports on Polar and Marine Research* 315, 145-259, doi: 10.2312/BzP_0315_1_1999

Siegert, C., Schirrmeister, L., and Babiy, O. (2002). The sedimentological, mineralogical and geochemical composition of late Pleistocene deposits from the ice complex on the Bykovsky peninsula, northern Siberia, *Polarforschung* 70, 3-11, doi: 10.2312/polarforschung.70.3

Stapel, J.G, Schwamborn, G., Schirrmeister, L., Horsfield, B. and Mangelsdorf, K. (2018). Substrate potential of last interglacial to Holocene permafrost organic matter for future microbial greenhouse gas production. *Biogeosciences* 15, 1969–1985, doi: 10.5194/bg-15-5423-2018

Walz, J., Knoblauch, C., Tigges, R., Opel, T., Schirrmeister, L., and Pfeiffer, E.-M. (2018) Greenhouse gas production in degrading ice-rich permafrost deposits in northeast Siberia. *Biogeosciences* 15, 5423–5436, doi: 10.5194/bg-2018-225

Wetterich, S., Schirrmeister, L., and Pietrzeniuk, E. (2005). Freshwater ostracodes in Quaternary permafrost deposits from the Siberian Arctic. *Journal of Paleolimnology* 34, 363-376. doi: 10.1007/s10933-005-5801-y

Wetterich, S., Kuzmina, S., Andreev, A.A., Kienast, F., Meyer, H., Schirrmeister, L., Kuznetsova, T., and Sierralta, M. (2008). Palaeoenvironmental dynamics inferred from late Quaternary permafrost deposits on Kurungnakh Island, Lena Delta, Northeast Siberia, Russia. *Quaternary Science Reviews* 27, 1523-1540, doi: 10.1016/j.quascirev.2008.04.007

Wetterich, S., Schirrmeister, L., Andreev A. A., Pudenz, M., Plessen, B, Meyer, H., Kunitsky, V. V. (2009). Eemian and Late Glacial/Holocene palaeoenvironmental records from permafrost

sequences at the Dmitry Laptev Strait (NE Siberia, Russia). *Palaeogeography, Palaeoclimatology, Palaeoecology* 279, 73-95, doi: 10.1016/j.palaeo.2009.05.002

Wetterich, S., Rudaya, N., Meyer, H., Opel, T., and Schirrmeister, L. (2011). Last Glacial Maximum records in permafrost of the East Siberian Arctic. *Quaternary Science Reviews* 30, 3139-3151, doi: 10.1016/j.quascirev.2011.07.020

Wetterich, S., Rudaya, N., Andreev, A.A., Opel, T., Schirrmeister, L., Meyer, H., and Tumskoy, V. (2014). Ice Complex formation in arctic East Siberia during the MIS3 Interstadial. *Quaternary Science Reviews* 84, 39-55, doi: 10.1016/j.quascirev.2013.11.009

Wetterich, S.; Tumskoy:V.E., Rudaya, N., Kuznetsov, V., Maksimov, F., Opel T. , Meyer H., Andreev, A.A., and Schirrmeister, L. (2016). Ice Complex permafrost of MIS5 age in the Dmitry Laptev Strait coastal region (East Siberian Arctic). *Quaternary Science Reviews* 147, 298-31, doi: 10.1016/j.quascirev.2015.11.016

Wetterich, S., Rudaya, N., Kuznetsov V., Maksimov, F., T. Opel, Meyer, H., Guenther, F., Bobrov, A., Raschke, E., Zimmermann, H., Strauss, J., Fuchs, M.C., and Schirrmeister, L. (2019). Recurrent Ice Complex formation in arctic eastern Siberia since about 200 ka. *Quaternary Research* 92(2); 530-548, doi: 10.1017/qua.2019.6

Wetterich. S., Fritz; M., Meyer, H., Mollenhauer, G., Rethemeyer, J., Kizyakov; A., Schirrmeister, L., and Opel, T. (2021). Northeast Siberian permafrost ice-wedge stable isotopes depict pronounced Last Glacial Maximum winter cooling. *Geophysical Research Letter* 48(7), e2020GL092087, doi: 10.1029/2020GL092087

Winterfeld, M., Schirrmeister, L., Grigoriev, M., Kunitsky, V.V., Andreev, A., and Overduin, P.P. (2011). Permafrost and Landscape Dynamics during the Late Pleistocene, Western Laptev Sea Shelf, Siberia. *Boreas* 40(4), 697–713, doi: 10.1111/j.1502-3885.2011.00203.x

Zimmermann, H.H., Raschke, E., Epp, L.S., Stoof-Leichsenring, K.R., Schirrmeister, L., Schwamborn, G., and Herzschuh, U. (2017). The history of tree and shrub taxa on Bol'shoy Lyakhovsky Island (New Siberian Archipelago) since the last interglacial uncovered by sedimentary ancient DNA and pollen data. *Genes* 8(10), E273; doi: 10.3390/genes8100273

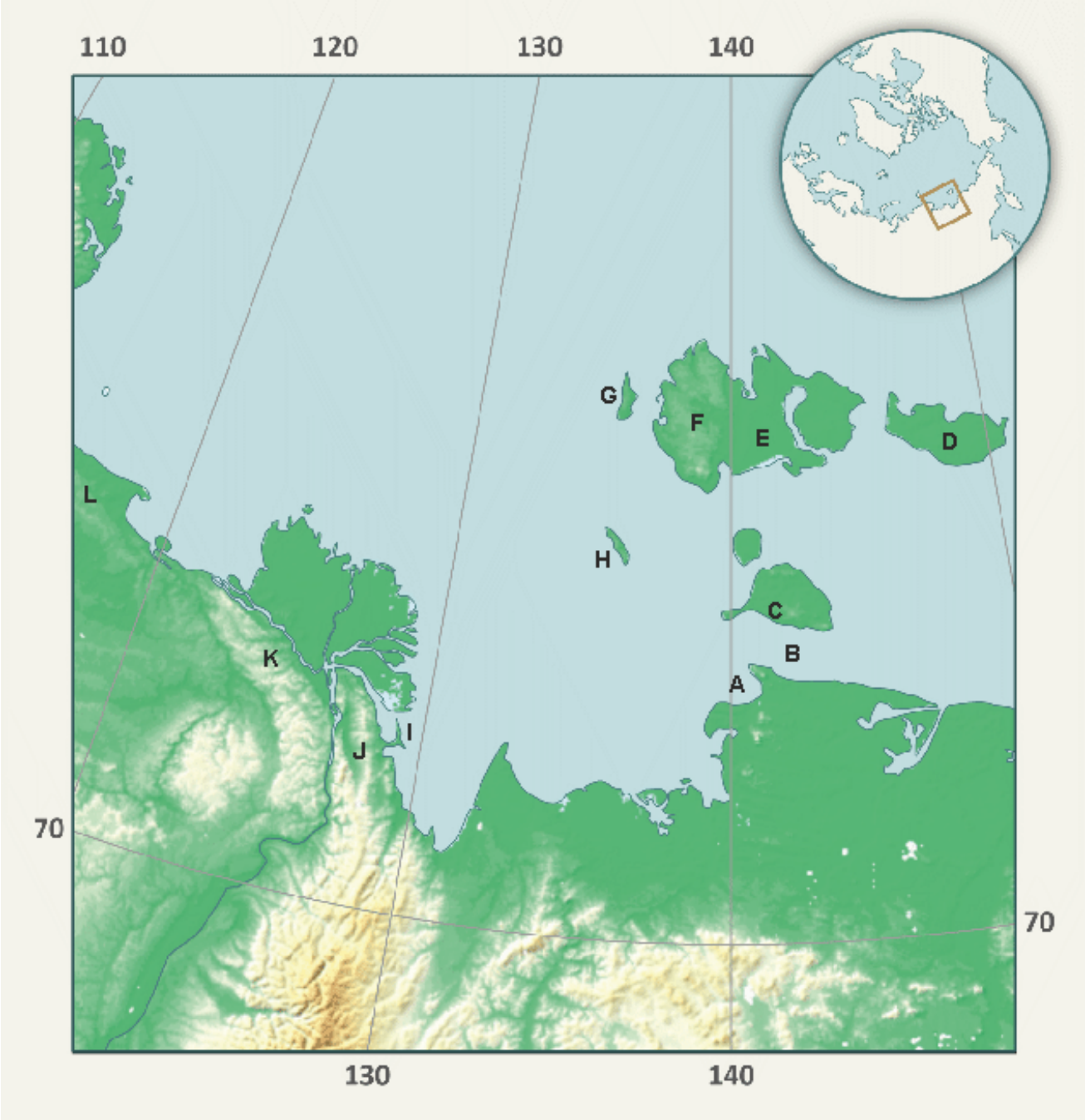

Supplementary Figure 1. Important landscape elements used in the paper. A – Granite domes of Cape Svyatoy Nos, B – Dmitrii Laptev Strait, C – Khaptagai Tas Hill on Bol'shoy Lyakhovsky Island, D – Novaya Sibir Island, E - Bunge Land, F – Kotel'ny Island, G – Bel'kovsky Island, H – Stolbovoy Island, I – Bykovsky Peninsula, J - Kharaulakh Range, K – Chekanovsky Ridge, L - Pronchshishev Ridge

Supplementary Table S2. Description of heavy and light minerals in each stratigraphic unit

No	Site	Descriptions
1	Bol'shoy Lyakhovsky Island	**MIS >7 (Cryogenic Eluvium)** - Grains are weakly rounded and clean. - Rhombic pyroxene is represented by hypersthene. - Hornblende is dark green, rarely brown. - Garnet (almandine) is pink, sometimes corroded, with numerous ore inclusions. - Sphene and ilmenite are partially leucoxenized. - Tourmalines are columnar, blue, pink, brown, and green with strong pleochroism. - Zircons are prismatic bipyramidal. - Feldspars are unrounded and weakly rounded, altered (sericitized, slightly ferruginous), or fresh; remnants of sandstones cement. – detritus rock grains are translucent or translucent at the edges. **MIS 7 (Yukagir)** **-** Grains are unrounded and weakly rounded. - Epidote: Along with transparent debris of pistachio green color, aggregated fragments are present. small amount of zoisite. - Monoclinic pyroxenes: weakly colored and colorless diopside in good preservation; rhombic pyroxenes are hypersthene. - Amphiboles are dark green, rarely brown, and nearly colorless. - Quartz (unrounded) and feldspars are contaminated with iron-humus stains and often occur in intergrowths. - Feldspars are unrounded, partly chloritized. - Carbonate aggregates are ferruginous. **MIS 6 (Zimov'e Stratum)** - Grains are clear, iron-free and unrounded or weakly rounded. - Epidote is of variable preservation. - Ilmenite and anatase are partially leucoxenized. - Leucoxene as dense grains with smooth surfaces. - Carbonates (calcite) are colorless and present in elongated crystals with distinct twinning and tangled-fibrous structure. **MIS 5e (Krest Yuryakh)** - Grains are angular, and subrounded. - Iron hydroxide grains of yellowish-ochre, reddish-brown, and almost black color. - Light fraction is dominated by sericitized feldspars. - Ilmenite is partially leucoxenized. - Epidote as irregular pistachio green fragments, in aggregates with other minerals. Zoisite is present in small amounts. - Rhombic pyroxenes are represented by hypersthene and enstatite. Enstatite as fragments of prismatic crystals, with distinct cleavage cracks, slightly greenish and colorless. - Hornblende is dark green, slightly rounded. - Mica plates are carbonated and ferruginous. - Calcite colorless or brown and micro-oolithic. - Magnetite on plant remains. **MIS 5a-d (Kuchchuguy, Buchchagy)** - Grains are weakly rounded or unrounded. - In the heavy mineral fractions rounded mica plates of different preservation dominated. - Ilmenite: angular, partially leucoxenized. - Epidote: well-formed prismatic crystals and fragments, good preservation. - Hornblende: elongated round grains of dark green color. - Sphene is crystalline and aggregated

		- Feldspars are unrounded or slightly rounded. - Iron hydroxides are compact, rounded grains. - Carbonates: rhomboedric, mirodrusses, white spherical aggregates (micro-oolithes). - Many grains are coated with an iron film. - Aggregates consist of clayey, micaceous particles and small fragments of various minerals, light colored. - Organo-mineral pellets are found containing carbonates and are reactive to iron and manganese. **MIS 4 (Zyryan)** - Grains are differently rounded and also angular. - Ilmenite is partially leucoxenized. - Epidote and pyroxene grains with fresh chipping. - Sphene is crystalline and aggregated. - Biotite as thin round plates of different preservation. - Feldspars are variably rounded. **MIS 3 (Kargin)** - Grains are only weakly rounded; most of them have a brownish film on the surface. - Predominant minerals are epidote and amphibole. - Light fraction consists of organo-mineral aggregates with admixture of feldspars, muscovite, and chlorite. - Carbonates are ferruginous, micro-oolithic. **MIS 2 (Sartan)** - high contents of plant detritus and clay material. - no detailed description. **MIS 1 (Holocene)** - Grains are angular. - Pyroxenes and amphiboles with fresh fragments and in aggregates with other minerals, ferruginous, chloritized. - Epidote is fresh and altered. - Anatase is represented by zonal bipyramidal crystals.
2	Oyogos Yar coast	**MIS 5e to 3 (Krest Yuryakh, Buchagy, Zyrayan, Kargin)** - Grains are weakly rounded or angular. - Epidote is of variable preservation, small amounts of zoisite are present. - Monoclinic pyroxene is represented mainly by diopside. - Rhombic pyroxenes (hypersthene) are rarely present. – Amphiboles are dark green, more rarely brown and light green. - Often garnet, epidote, and ilmenite in intergrowths with feldspars. - Titaniferous minerals are partially leucoxenitized. - Authigenic parts contain some fine-grained aggregates with iron-carbonate composition. - Carbonates are kidney-shaped and microdruses.
3	Cape Svyatoy Nos	**MIS 7 (Yukagir), MIS 5a-d (Kuchchuguy, Buchchagy), MIS 3 (Kargin)** - Grains are mostly angular and consist often of mineral aggregates. - Pyroxenes and amphiboles are partially chloritized and iron-bearing, Hornblende predominates; Monoclinic pyroxenes are diopsides. - unrounded, unaltered plagioclases predominate. - Carbonates are micro-ooliths.
4	Stolbovoy Island	No descriptions available
5	Bel'kovskiy Island	No descriptions available
6	Cape Anisii (Kotelny Island)	No descriptions available
7	Bunge Land	**MIS 2 (late Sartan), MIS 1 (Holocene)** - Grains of heavy fractions are well-rounded and preserved.

		- Ilmenite is often leucoxenized and intergrown with feldspars. - Epidotes are fragments of irregular shape, transparent to cloudy. - Monocline pyroxenes consist of colorless and light green diopside, more rarely of augite; sample Bun-7-1(lower terrace) is characterized by a great diversity in the composition of the occurring diopsides (bluish-green, emerald-green, light green, colorless); all grains are well preserved and show no traces of alteration. - The amphiboles belong to the ordinary hornblendes. Most often they have dark green, almost black color, rarely occur brown and almost colorless varieties. Sample Bun-7-1 is distinguished by the great variety of hornblendes. Bluish-green, dark green, almost black, dark brown, and brownish-green varieties occur. - Sample Bun-8 (lower terrace) contains 11.6% heavy minerals in the 63-125 μm fraction and 3.1% in the 125-250 μm fraction; in addition, the 63-125 μm fraction contains pyrite (grains of grape-like form or as crusts, partly somewhat oxidized to FeOOH, bronze-colored with partly distinct metallic luster).
8	Novaya Sibir Island	No descriptions available
9	Bykovsky Peninsula, Mamontovy Khayata,	**MIS 3 (Kargin), MIS 2 (Sartan), MIS 1 (Holocene)** - Mineral grains are slightly rounded or angular. - The heavy mineral composition in both investigated fractions is dominated by minerals of the pyroxene and amphibole groups. - The pyroxene group consists mainly of greyish brown augite with rare occurrence of diopsite and hypersthene in minor amounts. - The amphibole group is dominated by ordinary green colored hornblende. In addition, soda amphibole was sometimes observed. - Ilmenite, leucoxene, and epidote are present in significant amounts, followed by garnet, apatite, and sphene. - Zircon and tourmaline are continuously observed in minor amounts. - In small but marked amounts some sediments contain rutile, disthen, chloritoid, staurolith, and andalusite. - Some amounts of chlorite also occur in most samples. - Weathered mica is less frequently present. - A striking fact is the predominance of angular, fresh quartz grains in the light fraction. - Angular intergrowths of pyroxene, amphibole, and opaque minerals occur. - Aggregation of these minerals with feldspars can be also observed. - Augite and hornblende are mainly untouched and only a minor part shows signs of weathering (limonitisation, irregular coloring). - Different states of weathering suggest that source rocks were already partly transformed.
10	Bykovsky Peninsula, Bykovsky North	**MIS 3 (Kargin), MIS 2 (Sartan)** - In all samples except for B-S1 grains are not rounded and show frequent intergrowths of several minerals. - Monoclinic pyroxene in sample B-S1 is augite and diopside; in all other samples pyroxene is augite only. - Amphibole is ordinary hornblende; in sample B_S1 light green, dark green, and brown; in all other samples dark green only. - Feldspar predominantly as potassium feldspar, often cloudy.
11	Bykovsky Peninsula, Ivashkina Lagoon	**MIS 3 (Kargin), MIS 2 (Sartan), MIS 1 (Holocene)** - All samples are characterized by low yield of heavy fraction, unrounded terrigenous material, insignificant ore mineral content or lack thereof, and uniform mineralogical composition. - More diverse composition was sampled at the 6.11-6.13 m depth and at the 5.30-5.34 m depth. - Monoclinic pyroxenes are represented by gray-brown augite; a minor amount of light green diopside is present. Amphiboles are represented by dark green hornblende. - The light fraction is represented by feldspars, clasts of chlorite schists, sedimentary rocks, and aggregate grains.

		- In sample iv-2-99 (1.44-1.46 m depth), the light fractions of both fractions consist of unstable light gray fine aggregates; quantitatively, they account for 100%. In the heavy fractions of sample iv-2-99 (4.11-4.15 m), pyroxenes and amphiboles are partially fractured, ferruginous. - Many rock fragments, reddish brown ferruginous carbonate grains in dense aggregation (probably micro concretions). The carbonates are ferruginous. Their color is reddish-brown and yellow-brown. - The light fractions of samples 17/8, 10/3, and 15/5 have a composition similar to that of sample iv-2-99 (1.44-1.46 m).
12	Khorogor Valley	**MIS 1 (Holocene, modern)** - Samples have the same mineralogical composition, but different quantities of terrigenous material. - They contain rock fragments - predominantly fragments of chloritic shales, with a small amount of sedimentary and metamorphic rock fragments. - Predominant minerals in the heavy fraction are pyroxenes (augite) and, in some samples, titaniferous minerals (ilmenite, leucoxene, sphene, rutile). - In the light fractions feldspars predominate, which are mostly altered, turbid. - Samples rich in humus and iron hydroxides are brown colored (film on the surface and fillings on cleavage cracks). - Silty samples contain many unstable, easily disintegrated organominerals. - All minerals are angular, unrounded; in fluvial sediments only some grains are rounded and semi-rounded. Very often the grains occur as clusters of several minerals (ilmenite and augite, leucoxene and sphene, feldspars with minerals of the heavy fraction, etc.). - The amount of the heavy fraction is low.
13	Eastern Ebe Basyn Island	**MIS 2 (Sartan); MIS 1 (Holocene)** - The rounding of grains is weak, some of the grains are angular. - Rhombic pyroxenes are represented by hypersthene, enstatite grains are rare; monoclinic pyroxenes are represented by diopside and augite. - Most epidote grains are dark, and consist of fresh crystal fragments; zoisite is rarer. - Ilmenite is partially leucoxenized. - Zircons have an oval-elongated pomegranate shape and are bipyramidal. - In sample Ebe 4-11 grains are calcified, garnet is weakly calcified and angular; epidote grains are intergrown with hornblende.
14	Turakh Island	**MIS 3 (Kargin), MIS 2 (Sartan), MIS 1 (Holocene)** - Most grains are angular or weakly rounded; often there are clusters of two and three minerals. - Ilmenite is partially leucoxenized. - Epidote is more often opaque with secondary alteration products. - Aggregations of several minerals often occur: e.g. of pyroxene with feldspars, zircon with garnet, epidote with chlorite, garnet with epidote, sphene with rutile, ilmenite with feldspars and others. - Rhombic pyroxenes consist of hypersthene. Monoclinic diopsites have colorations of different intensity, rarely augite occurs. - Garnet is completely unrounded. - Titanium minerals (ilmenite, sphene) are often leucoxenitized. - Fe-bearing carbonates were considered as new formations (probably siderite), colorless calcite crystals are rare. Fe hydroxides occur in the form of rounded rearrangement products. - In sample T-02-1 are semi-rounded grains. Leucoxene develops on sphene and anatase. There are aggregates of pyroxene with hornblende: sphene is represented by flat, envelope-shaped crystals. - In samples T-021-6, T-021-10, T-021-11 mineral grains are covered with iron skins.
15	Nagym (southern Ebe Basyn Island)	**MIS 3 (Kargin)** - Grains with different roundness. Some minerals are fissured with black and brown parts. -- Ilmenite is often leucoxedized. - Epidote is clear and dark, zoisite occurs intergrown with hornblende and feldspar. - Pyroxenes (diopside and augite) are colorless or brown and are present in aggregates with feldspar, sometimes ferruginous. Enstatite is present among the rhombic pyroxenes.

		- Amphibole is clear and dark with a fractured surface, sometimes contaminated with clayey material. - Garnets are colorless, pink, and brown; grains are angular and in aggregates with hornblende and epidote. - Zircon is colorless and brownish. - Staurolite with carbonaceous inclusions. - Chlorite is intergrown with ilmenite interspersed with rutile needles.
16	Khardang Sise Island	**MIS 3 (Kargin), MIS 2 (Sartan)** - The heavy mineral association corresponds to Turakh Island above. - Ilmenite grains are leucoxenized. - The light fraction of the Kha-2-11, 2-28, 2-33 samples are calcified and weakly rounded. - Quartz grains are intergrown with rutile. - Feldspars are contaminated and have black spotty inclusions. - Microaggregate carbonates are part of organomineral aggregates.
17	Kurungnakh Island	**MIS 3 (Kargin), MIS 1 (Holocene)** - There are clear differences between the Lower Sand Unit (MIS 3 S) and the covering Ice Complex Unit (MIS 3 IC). - This is especially reflected in higher garnet and epidote contents as well as lower pyroxene and amphibole contents of the Ice Complex deposits - The heavy mineral composition of the Lower Sand Unit is comparable to all the other samples from the Lena Delta.
18	Cape Mamontov Klyk	**MIS 3 (Kargin), MIS 2 (Sartan), MIS 1 (Holocene)** - All samples are rather uniform in composition and mineral appearance. - The grains are differently rounded; weakly rounded grains dominate. The preservation of the grains is good, except for epidote and micas. - The predominant minerals of the heavy fraction are epidote, pyroxene, and amphibole. - Ilmenite is rounded and weakly rounded, sometimes leucoxenized. Sometimes it is found in assemblages with sphene. - Epidote is usually in the form of irregularly shaped fragments, and clouded by secondary alteration products. Less common are prismatic crystals of good preservation. Sometimes epidote grains are found in aggregates with other minerals (e.g., zoisite). - Monoclinic pyroxenes are represented by colorless and light green diopside grains. Augites are present as a minor admixture; sometimes the ratio of augites and diopside changes. - Rhombic pyroxenes are represented by hypersthene. - Amphiboles are represented by dark green, rarely by brown hornblende. - Garnets are irregularly shaped, weakly rounded, colorless to pink (almandine). Rarer are brown, orange, and bright yellow varieties. - Zircon is found as prismatic-bipyramidal crystals and their fragments. - Tourmaline occurs as prismatic crystals and their fragments. Their coloration is brown (magnesian variety) or more rarely blue (ferruginous variety). - Sphene occurs in the form of prisms and envelope-like flattened crystals, but more often as irregular fragments and aggregate grains, often leucoxenized. The coloration of the grains varies from light brown to intense brown, reddish, with strong pleochroism. - Rutile is partially leucoxenized. - Mica is ferruginous and fissured. - Hydrous iron oxides are often found as spherical formations. They are probably ferruginous marcasite. - Carbonates (calcite) are colorless, irregularly shaped fragments, more rarely prismatic crystals, micro-oolites, rosettes are found.

Supplementary Table S3. Excel file of the mean contents of heavy and light mineral composition for the 63-125 µm and the 125-250 µm fraction for each study site and each studies horizon

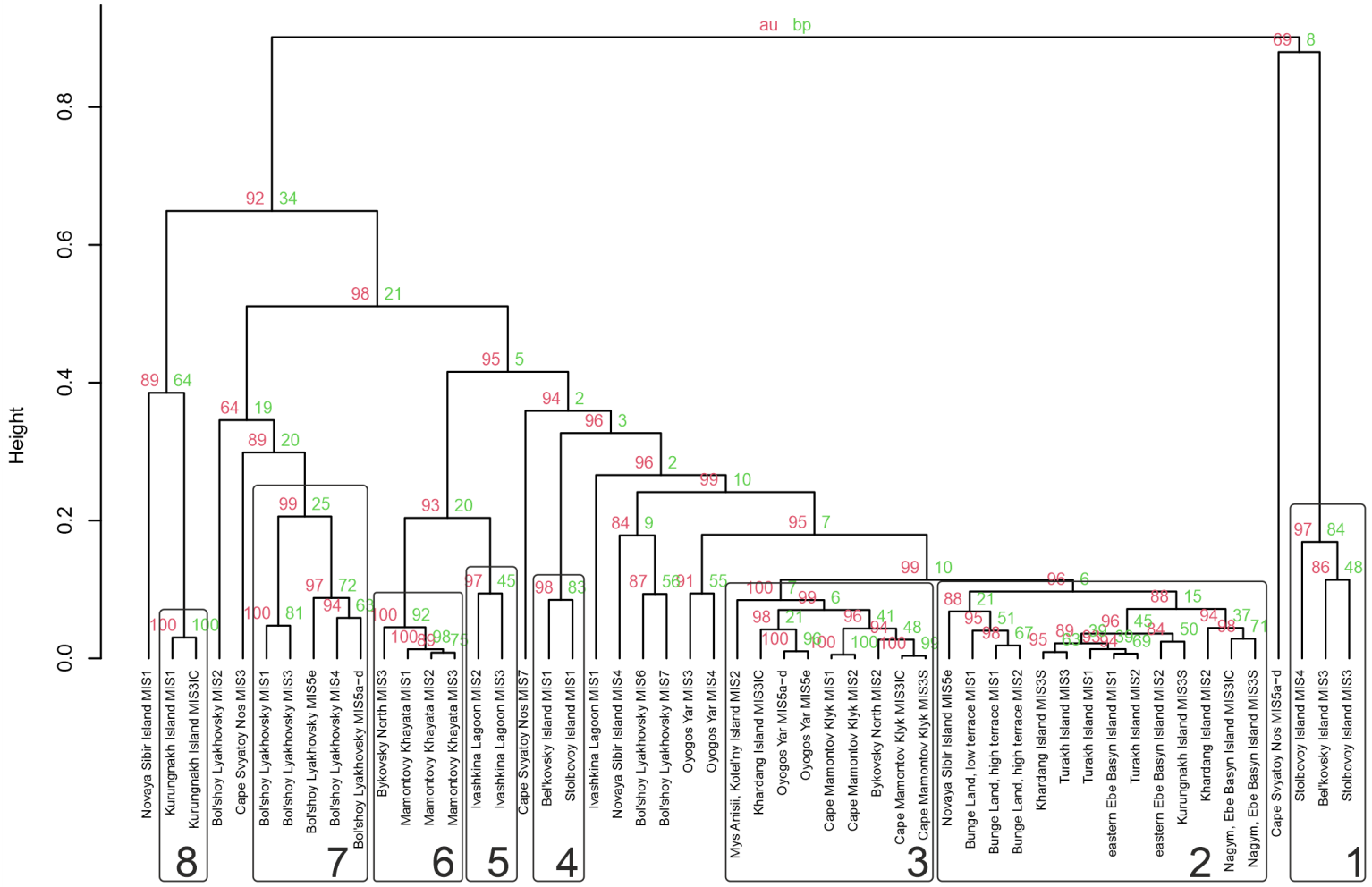

Supplementary Figure S2. Cluster dendrogram for the hierarchical clustering of heavy mineral association sample means (fine fraction) for each age and sample site. Distances between site/age combinations are assessed using the chi-squared method. Clustering method is "average". Clusters are indicated by black rectangles. Numbers at the dendrogram edges are for basic bootstrapping probability significance values (red) and corrected approximately unbiased significance values (green), statistical significances according to the bootstrapping approach used in the pvclust package.

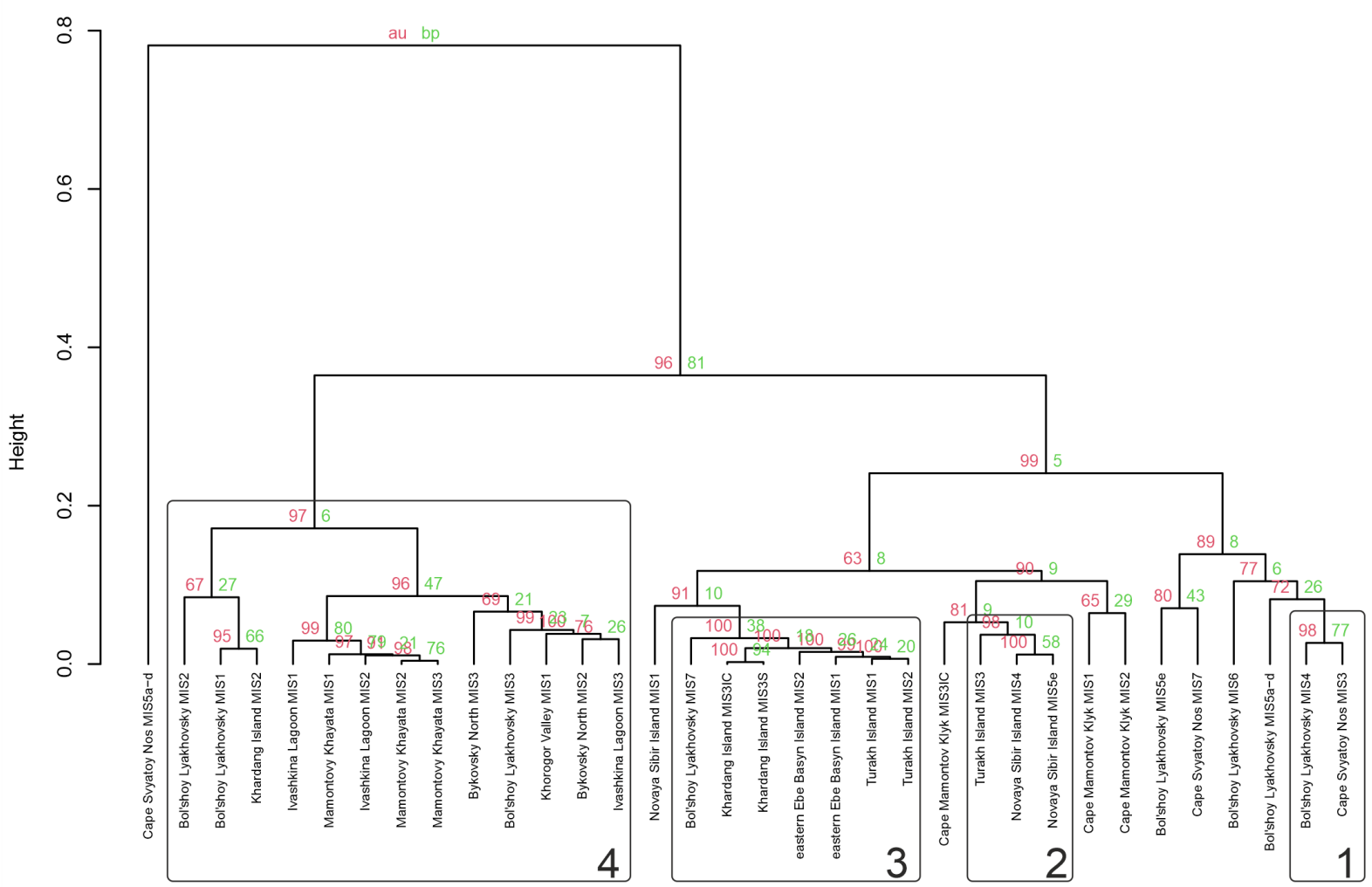

Supplementary Figure S3. Cluster dendrogram for the hierarchical clustering of light mineral association sample means (fine fraction) for each age and sample site. Distances between site/age combinations are assessed using the chi-squared method. Clustering method is "average". Clusters are indicated by black rectangles. Numbers at the dendrogram edges are for basic bootstrapping probability significance values (red) and corrected approximately unbiased significance values (green), statistical significances according to the bootstrapping approach used in the pvclust package.